

## Supplementary information

### **Penetrating Chains Mimicking Plant Root Branching to Build Mechanical Robust, Ultra-stable CO<sub>2</sub>-philic Membranes for Superior Carbon Capture**

Xu Jiang, Shanshan He, Songwei Li, Yongping Bai, and Lu Shao\*

MIT Key Laboratory of Critical Materials Technology for New Energy Conversion and Storage, State Key Laboratory of Urban Water Resource and Environment School of Chemistry and Chemical Engineering, Harbin Institute of Technology, Harbin 150001, PR China.

Email: [shaolu@hit.edu.cn](mailto:shaolu@hit.edu.cn)

### Gas permeation test.

**Pure gas permeation.** Pure gas permeation measurements were conducted on a home-made constant-volume apparatus using the time-lag method. The pure gas permeability ( $P$ ) with the unit of Barrer (1 Barrer =  $10^{-10}$  cm<sup>3</sup>(STP) cm / (cm<sup>2</sup> s cm Hg) can be expressed by the following Equation 1:

$$P = D \times S \quad (1)$$

Where  $D$  (cm<sup>2</sup>/s) is the diffusion coefficient (diffusivity),  $S$  (cm<sup>3</sup> (STP) / cm<sup>3</sup> cm Hg) represents the sorption coefficient (solubility). The ideal selectivity of gas A over gas B ( $\alpha_{a/b}$ ) is defined as the ratio of their permeabilities as Equation 2 shows:

$$\alpha_{\frac{A}{B}} = \frac{P_A}{P_B} = \left[ \frac{D_A}{D_B} \right] \times \left[ \frac{S_A}{S_B} \right] \quad (2)$$

The gases were tested in the sequence of H<sub>2</sub>, N<sub>2</sub>, and CO<sub>2</sub> under 35 °C and 3.5 atm. The gas permeability could be calculated by the following Equation 3:

$$P = \frac{273 \times 10^{10}}{760} \frac{Vl}{AT \left( p_2 \times \frac{76}{14.7} \right)} \frac{d_p}{d_t} \quad (3)$$

Where  $dp/dt$  is the steady increase rate of downstream-pressure,  $V$  is the volume of the downstream chamber (cm<sup>3</sup>),  $l$  is the membrane thickness (cm).  $A$  is the effective test area of the membrane (cm<sup>2</sup>),  $T$  is the operating temperature (K) and  $p_2$  is the upstream operating pressure (psi).

Using the diffusion time lag ( $\theta$ ) extrapolated from the plot of pressure with time at steady state to the time axis, the diffusivity can be calculated by Equation 4:

$$D = \frac{l^2}{6\theta} \quad (4)$$

The solubility can be simply deduced from Equation 1.

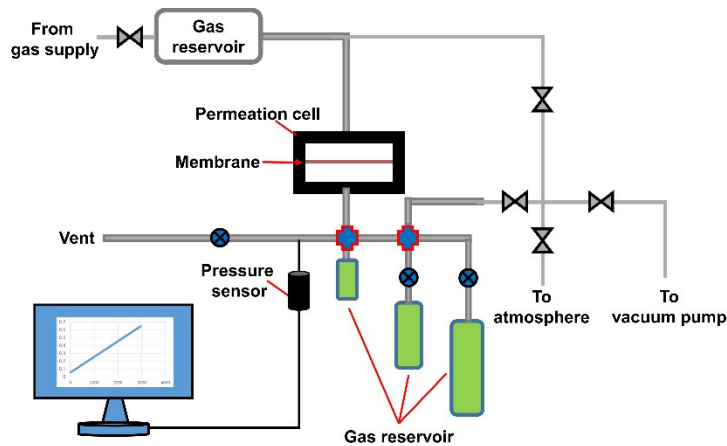


**Figure S1.** Home-made apparatus for pure-gas permeation test.

**Mixed gas permeation.** Mixed gas permeation properties of the membranes were investigated based on

a binary 50% CO<sub>2</sub> and 50% N<sub>2</sub> mixture under 35 °C and 7 atm feed pressure. To ensure constant gas molarity in the retentate, small amounts of retentate are slowly discharged into water or the atmosphere via a silicon piping. The sampling process was initiated by evacuating the line from the receiving volume (the lower chamber: downstream) to GC by vacuum pump. The compositions of the feed and permeate were analyzed by GC. The choice of carrier gas in the GC setup is nitrogen. Permeability of each gas can be determined using the following equations:

$$P_A = \frac{273 \times 10^{10}}{760} \frac{y_A \times V \times l}{AT(P_2 \times \phi_A \times (76/14.7) \times x_A)} \frac{dp}{dt} \quad (5)$$

$$P_B = \frac{273 \times 10^{10}}{760} \frac{y_B \times V \times l}{AT(P_2 \times \phi_B \times (76/14.7) \times x_B)} \frac{dp}{dt} \quad (6)$$

where  $P_A$  and  $P_B$  refer to the permeability of CO<sub>2</sub> and N<sub>2</sub> respectively.  $P_2$  symbolizes the upstream feed gas pressure (psi).  $x$  and  $y$  represent molar fractions of the gas in feed and permeate sides, respectively.  $\phi_A$ ,  $\phi_B$  indicate fugacity coefficients of respective gases in the upstream.

The mixed gas selectivity is expressed by the following equation:

$$\alpha_{\frac{A}{B}} = \frac{P_A}{P_B} \quad (7)$$

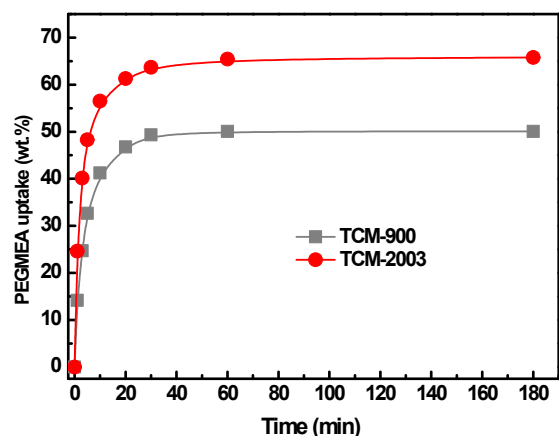


Figure S2. PEGMEA uptakes of TCM-900 and TCM-2003 over soaking time.

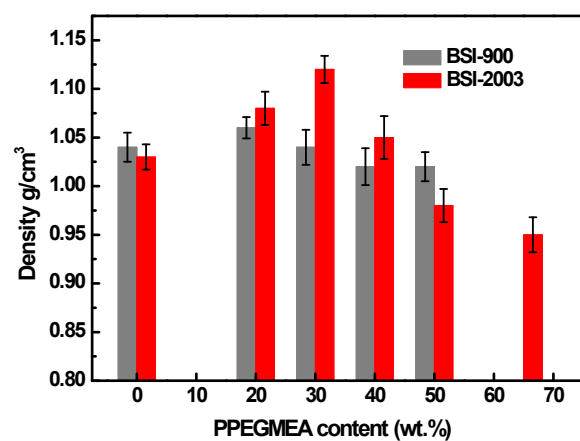


Figure S3. Densities of BSI-900 and BSI-2003 at different PEGMEA contents.

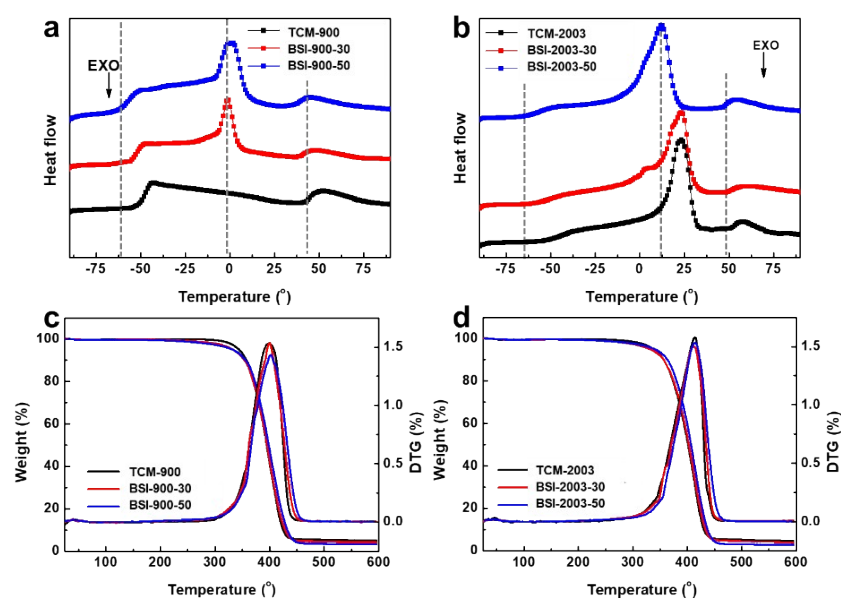
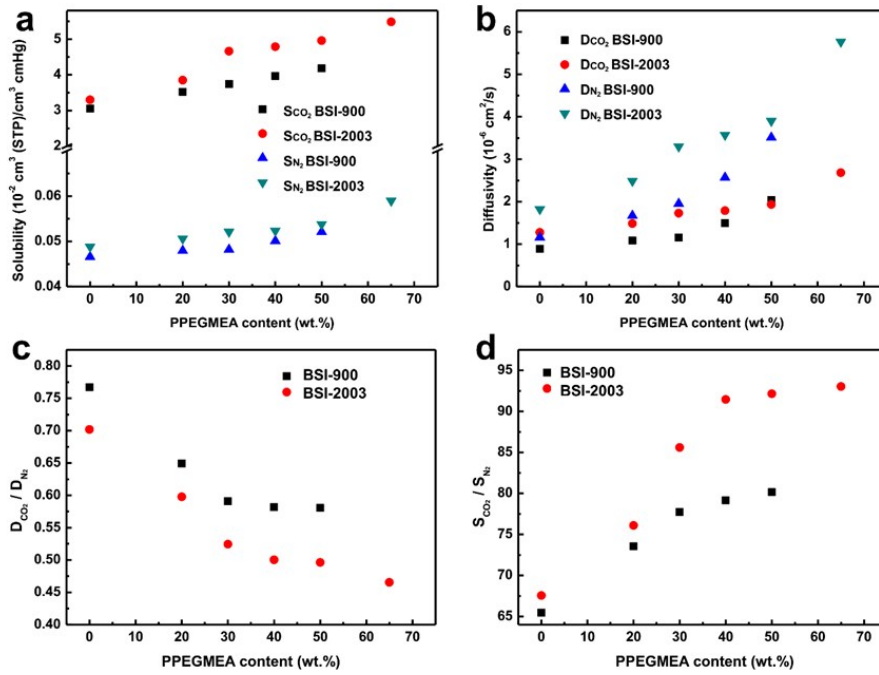
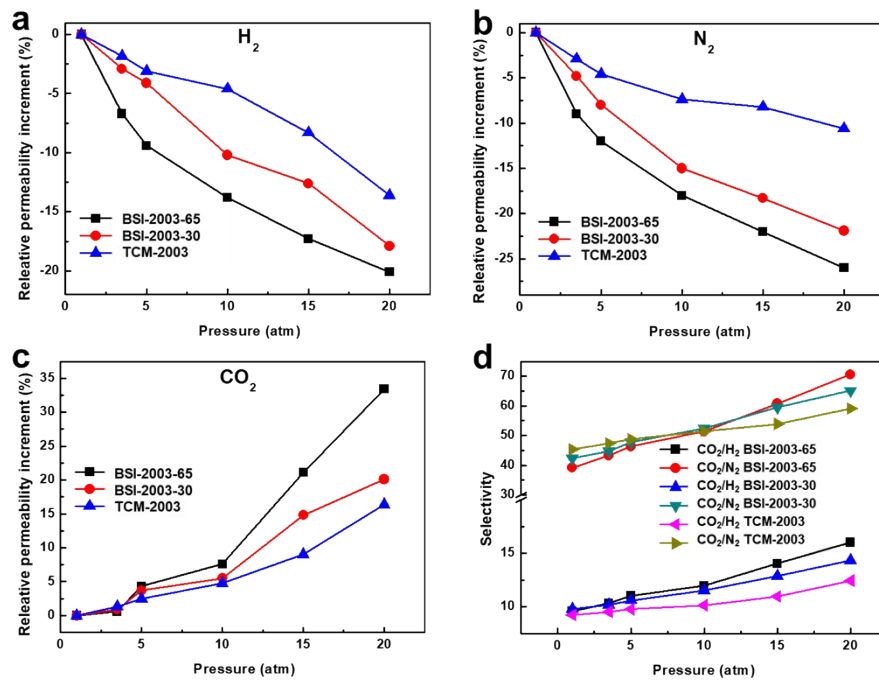


Figure S4. DSC thermograms, TGA and DTG curves of a,c) BSI-900 and b,d) BSI-2003



**Figure S5.** Solubility and diffusivity of a) BSI-900 and b) BSI-2003 as a function of PPEGMEA content. Diffusivity selectivity and solubility selectivity of c) BSI-900 and d) BSI-2003 as a function of PPEGMEA content.



**Figure S6.** a)  $\text{H}_2$ , b)  $\text{N}_2$  and c)  $\text{CO}_2$  permeability as well as d)  $\text{CO}_2/\text{N}_2$  and  $\text{CO}_2/\text{H}_2$  selectivity of BSI-2003 as a function of test pressure.

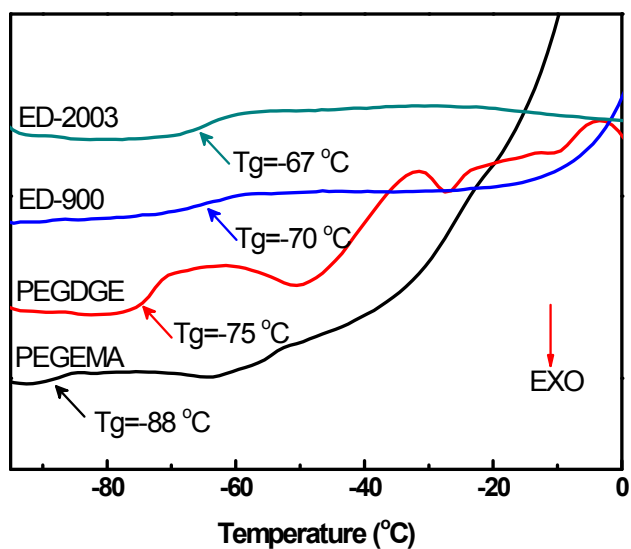


**Figure S7.** DSC results of PEO monomers.

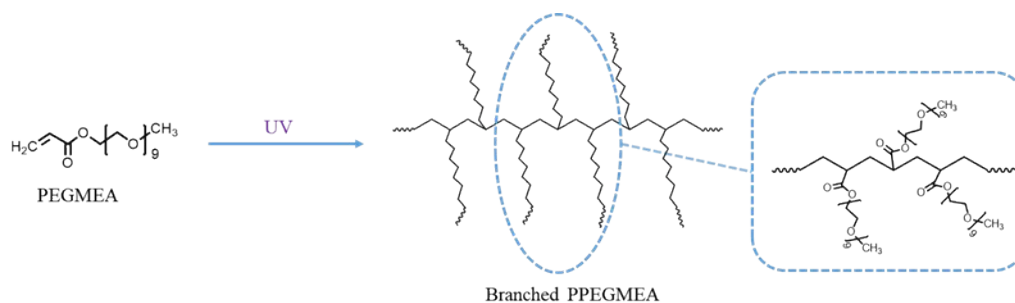


**Figure S8.** The polymerization of PEGMEA under UV irradiation

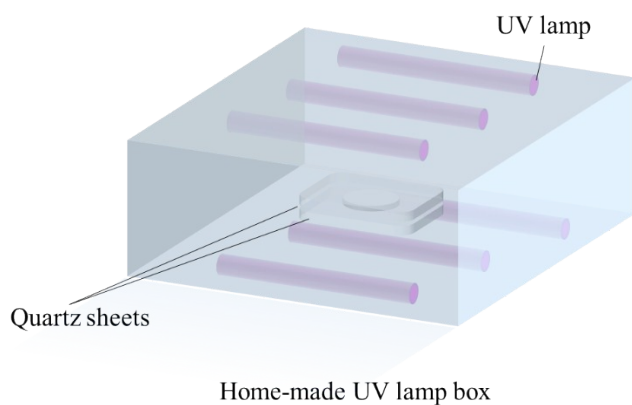


**Figure S9.** Illustration of the home-made UV lamp box

**Table S1.** Tensile strength and elongation at break of BSI-900 membranes

<b>Membrane</b>	<b>Elongation at break (%)</b>	<b>Tensile strength (Mpa)</b>
<b>TCM-900</b>	40.7	0.99
<b>BSI-900-20</b>	51.0	1.06
<b>BSI-900-30</b>	61.7	1.10
<b>BSI-900-40</b>	67.4	1.34
<b>BSI-900-50</b>	76.7	1.52

**Table S2.** Tensile strength and elongation at break of BSI-2003 membranes

<b>Membrane</b>	<b>Elongation at break (%)</b>	<b>Tensile strength (Mpa)</b>
<b>TCM-2003</b>	153.0	0.85
<b>BSI-2003-20</b>	169.3	0.96
<b>BSI-2003-30</b>	182.4	1.02
<b>BSI-2003-40</b>	202.6	1.20
<b>BSI-2003-50</b>	230.1	1.24
<b>BSI-2003-65</b>	233.4	1.35

**Table S3.** Permeability and selectivity of BSI membranes.

	PPEGMEA (wt.%)	Permeability (Barrer)			Selectivity	
		H <sub>2</sub>	CO <sub>2</sub>	N <sub>2</sub>	CO <sub>2</sub> /H <sub>2</sub>	CO <sub>2</sub> /N <sub>2</sub>
<b>BSI-900</b>	0	40	272	5.4	6.8	50.3
	20	42	384	8.0	9.1	48.0
	30	48	432	9.4	9.0	45.9
	40	63	593	12.9	9.4	46.0
	50	90	850	18.3	9.4	46.5
<b>BSI-2003</b>	0	44	422	8.9	9.5	47.4
	20	57	573	12.6	10.1	45.5
	30	76	772	17.2	10.2	44.9
	40	85	855	18.7	10.1	45.7
	50	91	960	21.0	10.5	45.7
	65.0	142	1473	34.0	10.3	43.3

**Table S4.** Mixed gas permeation data BSI-2003 membranes

	PPEGMEA (wt.%)	Permeability (Barrer)			Selectivity	
		H <sub>2</sub>	CO <sub>2</sub>	N <sub>2</sub>	CO <sub>2</sub> /H <sub>2</sub>	CO <sub>2</sub> /N <sub>2</sub>
<b>BSI-2003</b>	0	40	366	13	9.1	27.5
	30	79	733	22	9.3	34.1
	65.0	130	1252	36	9.6	35.2

**Table S5.** Tg values of TCM and BSI membranes

Membrane	Tg (°C)
<b>TCM-900</b>	-51
<b>BSI-900-30</b>	-54
<b>BSI-900-50</b>	-61
<b>TCM-2003</b>	-53
<b>BSI-2003-30</b>	-58



Table S6. EO content of PEO materials used in this work

Material	Structure	EO content (wt.%)
ED-900	$y = 12.5, (x+z) \approx 6$	56.6
ED-2003	$y = 39, (x+z) \approx 6$	80.3
PEGDGE	$m \approx 9$	75.3
PEGMEA	$m \approx 9$	82.5

**Table S7** Performance comparison of the CO<sub>2</sub>-philic membranes and BSI membranes in this work.

<b>Membrane</b>	<b>Test conditions</b>	<b>CO<sub>2</sub> permeability (barrer)</b>	<b>CO<sub>2</sub>/H<sub>2</sub></b>	<b>CO<sub>2</sub>/N<sub>2</sub></b>	<b>Ref.</b>
Semi-crystalline PEO	35 °C & 4 atm	12	6.7	48	[1]
Cross-linked PEO	35 °C & 3.5 atm	180	6.8	58	[2]
Cross-linked PEGDA	35 °C & 4 atm	110	7.3	50	[3]
PEO-PBT+PEG-DBE	30 °C & 0.3 atm	750	12.4	40.0	[4]
PEBAX®/PDMS-PEG (50 wt.%)	35 °C & 4 atm	532	10.6	36.1	[5]
Star-like PEO	35 °C & 2 atm	850		51	[6]
PEG cross-linked with A-amine 80% free PEGDME	25 °C & 2 atm	196		108.5	[7]
Semi-interpenetrating PEO	35 °C & 3 atm	90.3	5.8	40.2	[8]
PEG-Jeffamine (100% free PEGDME)	25 °C & 2 atm	196		54	[9]
50.9 wt.% PEG-embedded PEO	35 °C & 3.5 atm	558	9.1	55	[10]
PEOlated ladder-structured polysilsesquioxane	35 °C & 1 atm	1530	8.9	43.8	[11]
PEO/5-hydroxyisophthalic acid	25 °C & 1 atm	573		32.4	[12]
PEO-PBT/GO -065 (0.065 wt.% GO)	25 °C & 0.5 atm	143	12	73	[13]
Cross-linked PEO/UiO-66-MA (2 wt.%)	35 °C & 3.5 atm	942	10.1	48.1	[14]
PDMS	35 °C & 1 atm	3800	4.3	9.5	[15]
PIM-1	25 °C & 4 atm	3054	1.7	16.1	[16]
BSI-900-50	35 °C & 3.5 atm	850	9.4	46.5	
BSI-2003-65	35 °C & 3.5 atm	1473	10.3	43.3	This
BSI-2003-65	35 °C & 10 atm	1574	12.0	51.4	work
BSI-2003-65	35 °C & 20 atm	1952	16.0	70.4	

## Reference:

- [1]. H. Lin and B. D. Freeman, *J. Membr. Sci.*, 2004, 239, 105-117.
- [2]. L. Shao, S. Quan, X.-Q. Cheng, X.-J. Chang, H.-G. Sun and R.-G. Wang, *Int. J. Hydrogen Energy*, 2013, 38, 5122-5132.
- [3]. H. Lin and B. D. Freeman, *Macromolecules*, 2006, 39, 3568-3580.
- [4]. W. Yave, A. Car, S. S. Funari, S. P. Nunes and K.-V. Peinemann, *Macromolecules*, 2010, 43, 326-333.
- [5]. S. R. Reijerkerk, M. H. Knoef, K. Nijmeijer and M. Wessling, *J. Membr. Sci.*, 2010, 352, 126-135.
- [6]. H. Zhao, X. Ding, P. Yang, L. Li, X. Li and Y. Zhang, *J. Membr. Sci.*, 2015, 489, 258-263.
- [7]. H. Zhao, X. Ding, P. Yang, L. Li, X. Li and Y. Zhang, *J. Membr. Sci.*, 2015, 489, 258-263.
- [8]. G. K. Kline, Q. Zhang, J. R. Weidman and R. Guo, *J. Membr. Sci.*, 2017, 544, 143-150.
- [9]. J. Deng, Z. Dai, J. Yan, M. Sandru, E. Sandru, R. J. Spontak and L. Deng, *J. Membr. Sci.*, 2019, 570-571, 455-463.
- [10]. S. Quan, Y. P. Tang, Z. X. Wang, Z. X. Jiang, R. G. Wang, Y. Y. Liu and L. Shao, *Macromol. Rapid Commun.*, 2015, 36, 490-495.
- [11]. S. Park, A. S. Lee, Y. S. Do, S. S. Hwang, Y. M. Lee, J. H. Lee and J. S. Lee, *Chem. Commun*, 2015, 51, 15308-15311.
- [12]. K. W. Yoon and S. W. Kang, *Chemical Engineering Journal*, 2018, 334, 1749-1753.
- [13]. M. Karunakaran, R. Shevate, M. Kumar and K. V. Peinemann, *Chem. Commun.*, 2015, 51, 14187-14190.
- [14]. X. Jiang, S. Li, S. He, Y. Bai and L. Shao, *J. Mater. Chem. A*, 2018, 6, 15064-15073.
- [15]. T. C. Merkel, V. I. Bondar, K. Nagai, B. D. Freeman and I. Pinnau, *J. Polym. Sci. Pol. Phys.*, 2000, 38, 415-434.
- [16]. B. Ghalei, K. Sakurai, Y. Kinoshita, K. Wakimoto, Ali P. Isfahani, Q. Song, K. Doitomi, S. Furukawa, H. Hirao, H. Kusuda, S. Kitagawa and E. Sivaniah, *Nat. Energy*, 2017, 2, 17086.